

# Integrating clinical reasoning into large language model-based diagnosis through etiology-aware attention steering

Peixian Li<sup>a,1</sup>, Yu Tian<sup>a,1</sup>, Ruiqi Tu<sup>a</sup>, Chengkai Wu<sup>b</sup>, Jingjing Ren<sup>c</sup>, Jingsong Li<sup>a,b\*</sup>

<sup>a</sup> *Engineering Research Center of EMR and Intelligent Expert System, Ministry of Education, Key Laboratory for Biomedical Engineering of Ministry of Education, College of Biomedical Engineering and Instrument Science, Zhejiang University, Hangzhou, 310027, China.*

<sup>b</sup> *School of Intelligent Science and Technology, Hangzhou Institute for Advanced Study, University of Chinese Academy of Sciences, Hangzhou, 310024, China.*

<sup>c</sup> *General Practice Department, the First Affiliated Hospital, College of Medicine, Zhejiang University, Hangzhou 310003, China*

<sup>1</sup> These authors contributed equally to this work.

## \* Corresponding Author:

Jingsong Li is with College of Biomedical Engineering and Instrument Science, Zhejiang University, No. 38 Zheda Road, Hangzhou, Zhejiang, 310027, China

Tel: +86-571-87951564

Fax: +86-571-87951564

Email address: ljs@zju.edu.cn.

Email address of every author:

Peixian Li: lipeixian@zju.edu.cn

Yu Tian: tyler@zju.edu.cn

Ruiqi Tu: ruiqi\_tu@zju.edu.cn

Chengkai Wu: wuck@ucas.ac.cn

Jingjing Ren: 3204092@zju.edu.cn

Jingsong Li: ljs@zju.edu.cn

## Abstract

**Objective:** Large Language Models (LLMs) demonstrate significant capabilities in medical text understanding and generation. However, their diagnostic reliability in complex clinical scenarios remains limited. This study aims to enhance LLMs' diagnostic accuracy and clinical reasoning ability.

**Method:** We propose an Etiology-Aware Attention Steering Framework to integrate structured clinical reasoning into LLM-based diagnosis. Specifically, we first construct Clinical Reasoning Scaffolding (CRS) based on authoritative clinical guidelines for three representative acute abdominal emergencies: acute appendicitis, acute pancreatitis, and acute cholecystitis. Next, we develop the Etiology-Aware Head Identification algorithm to pinpoint attention heads crucial for the model's etiology reasoning. To ensure reliable clinical reasoning alignment, we introduce the Reasoning-Guided Parameter-Efficient Fine-tuning that embeds etiological reasoning cues into input representations and steers the selected Etiology-Aware Heads toward critical information through a Reasoning-Guided Loss function.

**Result:** On the Consistent Diagnosis Cohort, our framework improves average diagnostic accuracy by 15.65% and boosts the average Reasoning Focus Score by 31.6% over baselines. External validation on the Discrepant Diagnosis Cohort further confirms its effectiveness in enhancing diagnostic accuracy. Further assessments via Reasoning Attention Frequency indicate that our models exhibit enhanced reliability when faced with real-world complex scenarios.

**Conclusion:** This study presents a practical and effective approach to enhance clinical reasoning in LLM-based diagnosis. By aligning model attention with structured CRS, the proposed framework offers a promising paradigm for building more interpretable and reliable AI diagnostic systems in complex clinical settings.

**Keywords—**Large Language Model, Clinical Reasoning, Parameter-Efficient Fine-tuning, Auxiliary Diagnosis, Acute Abdominal Emergencies

## 1. Introduction

With the rapid advancement of large language models (LLMs), their application in supporting medical decision-making has become an emerging area of interest. Pretrained on vast amounts of biomedical literature and clinical records, LLMs have demonstrated the ability to process unstructured text, answer clinical questions, and even propose diagnostic hypotheses (Singhal et al., 2023). Existing studies have shown their potential utility in tasks including triage, report generation, and symptom recognition (Williams, Miao, et al., 2024).

However, despite their capacity to handle complex inputs and generate coherent responses that appear logical, LLMs still face significant limitations in real-world clinical applications. Specifically, they struggle to comprehensively collect and integrate critical information, adhere to guideline-based reasoning paths, and make diagnostic decisions that align with clinical reasoning principles (Hager et al., 2024). In contrast, physicians rely on a combination of history-taking, physical examination, laboratory tests, and radiology report to establish accurate diagnoses (Bhangu et al., 2015; Lankisch et al., 2015; Gallaher & Charles, 2022). Therefore, developing intelligent diagnostic models that can reliably integrate clinical information and reason over it is crucial for improving diagnostic efficiency and accuracy.

Several recent efforts have sought to enhance clinical reasoning in LLMs. For example, Kwon et al. (2023) formalized diagnostic reasoning into chain-of-thought prompts to facilitate clinical reasoning by encouraging rationale generation; Gao et al. (2025) incorporated structured knowledge graph paths into LLMs' workflows to improve diagnostic accuracy and reasoning ability; Hua et al. (2024) fine-tuned LLMs on reasoning-oriented datasets derived from traditional Chinese medicine. These approaches have made some progress in improving the interpretability and reliability of LLMs in specific clinical tasks. However, most of these frameworks primarily rely on prompt engineering or external enhancements and have not optimized the reasoning mode at the internal level of LLMs. This gap becomes particularly critical in complex diagnostic scenarios, where research indicates that LLMs hold significant potential to improve diagnostic accuracy when properly guided (Williams, Zack, et al., 2024; Shah-Mohammadi & Finkelstein, 2024). Wang et al. (2025) significantly improved GPT-4's primary diagnosis prediction by requiring explicit reasoning processes, and Goglia et al. (2025) evaluated LLMs on acute cholecystitis questions derived from the Tokyo Guidelines,

highlighting the potential of LLMs in real diagnostic tasks.

To address these limitations, it is essential to develop strategies that embed clinical reasoning within the model itself and supervise its internal behavior during training. Given the transformer-based architecture at the core of LLMs—where multi-head self-attention mechanisms capture contextual relationships and feed-forward layers store and retrieve learned knowledge—targeting the internal attention heads provides a promising opportunity for reasoning enhancement (Vaswani et al., 2017; Zheng et al., 2025). Recent studies have revealed that certain attention heads play a critical roles in reasoning and information retrieval. Wu et al. (2024) proposed the Needle-in-a-Haystack test to identify Retriever Heads and demonstrated their utility in reducing hallucination and improving reasoning consistency. Xiao et al. (2024) explored gating mechanisms to assess the impact of pruning specific heads on performance, and identified heads that are critical for reasoning and streaming operations. Building on these insights, researchers have begun developing specialized mechanisms to enhance model fidelity and performance by selectively manipulating attention heads. For instance, Huang et al. (2025) introduced control tokens through masked heads to improve output faithfulness, while Gema et al. (2024) proposed a contrastive decoding framework leveraging specific attention heads to reduce factual errors and hallucinations.

Inspired by these findings, we propose a novel Etiology-Aware Attention Steering Framework designed to enhancing LLM-based diagnosis through internal reasoning supervision. We focus on three clinically similar and frequently misdiagnosed acute abdominal emergencies—acute appendicitis, acute pancreatitis, and acute cholecystitis—and construct Clinical Reasoning Scaffolding (CRS) based on authoritative clinical guidelines. Patient records are annotated accordingly to embed etiological reasoning cues and highlight reasoning elements corresponding to CRS. We then develop an Etiology-Aware Head Identification algorithm to detect attention heads that exhibit strong alignment with etiological reasoning, providing intervention points within the model. Finally, during fine-tuning, we implement a reasoning-guided attention steering mechanism to steer these heads toward the annotated information, ensuring the model adheres to clinically valid reasoning paths throughout the diagnostic process. The main contributions of this work are as follows:

- 1) Internal reasoning enhancement in LLMs for medical diagnosis: We develop an Etiology-Aware Head Identification algorithm that enables precise localization of internal attention mechanisms critical for clinical reasoning, providing a novel intervention path for improving diagnostic efficiency and accuracy.
- 2) Attention steering to ensure critical information focus: We propose an input-level etiological reasoning cues embedding method and a targeted attention steering strategy, effectively guiding the model to focus on annotated reasoning elements during fine-tuning.
- 3) Integration and evaluation of reliable clinical reasoning: Through data annotation and a Reasoning-Guided Loss function, we integrate structured clinical reasoning within the model and evaluate the model's reasoning capability using the Reasoning Focus Score and Reasoning Attention Frequency.

The rest of the paper is organized as follows: Section 2 reviews related work on LLM-based diagnosis and reasoning enhancement. Section 3 introduces the proposed framework in detail, including CRS construction and dataset annotation, Etiology-Aware Head Identification and Reasoning-Guided Parameter-Efficient Fine-Tuning. Section 4 presents the experimental setup and results. Section 5 offers a detailed discussion. Section 6 concludes the paper.

## **2. Related work**

### *2.1. Enhancing Clinical Reasoning in LLMs*

Clinical reasoning refers to the cognitive process by which physicians analyze patient information and progressively arrive at a diagnosis. It serves as the cornerstone of accurate medical decision-making. Although LLMs have demonstrated impressive performance in various medical natural language processing tasks, their ability to perform clinical reasoning—namely synthesizing symptoms, identifying diagnostic clues, and inferring potential etiologies—remains a substantial challenge, particularly in high-risk scenarios characterized by overlapping symptomatology. Recent efforts to enhance the reasoning capabilities of LLMs can be broadly categorized into three major directions: prompt engineering, attention and latent space modulation, and knowledge integration strategies.

**Prompt Engineering:** Prompt design plays a pivotal role in shaping the reasoning path of LLMs. Chain-of-thought (CoT) prompts have been shown to facilitate stepwise reasoning and improve interpretability (Wei et al., 2022). For example, Savage et al. (2024) demonstrated that CoT-augmented prompts enabled GPT-4 to produce analytical diagnostic outputs that closely mimic human reasoning processes. Sonoda et al. (2024) designed structured templates to guide the model through summarization and reasoning phases, resulting in improved diagnostic performance. Wu et al. (2024) proposed a context-filling framework that injects relevant concepts from medical knowledge graphs as knowledge seeds into prompts, enhancing both answer accuracy and interpretability. While these works show that LLMs can simulate structured diagnostic logic via carefully engineered prompts, they remain limited to representation-level manipulation and lack internal alignment with real clinical etiological reasoning processes.

**Attention and Latent Space Modulation:** Researchers have begun exploring internal mechanisms to enhance LLM reasoning. Venkateswaran & Contractor (2025) proposed SpotLight, which dynamically amplifies attention to relevant tokens, enabling LLMs to better follow task-specific instructions. Shen et al. (2025) introduced the Heima framework, which semantically decodes the reasoning process from the final hidden states associated with reasoning-specific tokens, validating the feasibility of latent space reasoning. Hao et al. (2024) further advanced this idea by embedding final hidden states directly into subsequent token inference steps, enabling continuous latent reasoning and improving inference quality. Although these approaches show the promise of attention and latent space modulation, they lack integration with clinical traits and fall short of enabling trustworthy clinical reasoning in real-world diagnostic tasks.

**Knowledge Integration:** Another direct yet effective strategy involves updating model parameters using curated medical knowledge and reasoning-augmented datasets. For instance, MedReason builds reasoning chain datasets by combining knowledge graphs with public medical QA corpora, and uses them to fine-tune LLMs, significantly improving diagnostic logic and interpretability (J. Wu et al., 2025). Retrieval-augmented generation (RAG) methods have also been applied. Kresevic et al. (2024) retrieved and incorporated authoritative clinical guideline content during generation, enabling evidence-based reasoning outputs. Meanwhile, domain-specific pretraining efforts such as MedFound demonstrate that incorporating expert-annotated reasoning into training can enhance LLMs' ability to produce standardized and specialty-consistent diagnoses across clinical domains (Liu et al., 2025).

Compared to prompt-based approaches, our method not only utilizes task-specific prompts to motivate and capture the model's etiological reasoning ability but also actively supervises attention distribution during fine-tuning to align internal attention with reasoning cues and elements. While attention-based methods such as SpotLight have enabled dynamic attention modulation, we go a step further by introducing Etiology-Head Identification, which locates attention heads aligned with annotated reasoning elements and uses them to supervise model behavior, thereby embedding the etiology-aware capability. Moreover, our approach bridges the gap between internal attention manipulation and external clinical knowledge, providing a fine-grained mechanism to steer LLMs toward reasoning processes that are coherent with real-world diagnostic logic.

## 2.2. Parameter-Efficient Fine-Tuning

As the parameter scale of LLMs continues to grow, full-parameter fine-tuning has become increasingly computationally expensive and often impractical in resource-constrained or high-risk domains such as medicine. To address this challenge, a series of Parameter-Efficient Fine-Tuning (PEFT) methods have been proposed, among which Low-Rank Adaptation (LoRA) and its variants have emerged as particularly effective strategies (Ding et al., 2023; Hu et al., 2021). LoRA, along with variants like QLoRA and AdaLoRA, introduces trainable low-rank matrices into frozen transformer weights (Dettmers et al., 2023; Zhang et al., 2023). By updating less than 1% of parameters, it allows models to adapt to downstream tasks while achieving performance comparable to or better than full-parameter fine-tuning. Building upon this foundation, several studies have proposed enhancements to PEFT techniques to further improve LLMs' performance in the medical domain. For example, Xu et al. (2025) introduced STAF-LLM, which combines AdaLoRA with a task-guided router to selectively integrate knowledge from 12 medical experts. Yan et al. (2025) developed the STP training method, which leverages transformer preference for specific tokens, achieving near full-parameter fine-tuning performance on the GLUE benchmark by updating only 0.009% of the model parameters.

In our work, we adopt the LoRA approach for fine-tuning and integrate a novel Reasoning-Guided Loss function. Unlike

standard loss functions, our method operates at the attention layer level by penalizing the model when its attention weights neglect annotated reasoning elements. This guides the model to consistently focus on clinically key information throughout the decoding process, thereby aligning attention behavior with clinical reasoning.

### 2.3. Auxiliary Diagnosis Models for Acute Abdomen Emergencies

Existing studies have highlighted both the potential and limitations of auxiliary diagnostic models in emergency settings. For instance, Males et al. (2024) and Ma et al. (2025) observed that traditional models often fail to produce accurate predictions unless symptom inputs are appropriately structured and interpreted. Hager et al. (2024) developed a benchmark dataset (MIMIC-CDM) consisting of thousands of acute abdomen emergencies. Their evaluations revealed that general-purpose LLMs exhibit suboptimal performance in diagnosing conditions such as acute cholecystitis and acute pancreatitis, primarily due to their limited ability to integrate structured clinical data and adhere to guideline-based reasoning processes. To address these challenges, researchers have proposed innovations tailored to real-world clinical diagnostic workflows. Li et al. (2025) addressed the issue of LLMs overlooking key diagnostic information and lacking confirmatory logic by constructing a stepwise fine-tuning dataset aligned with real clinical workflows (history taking → physical exam → diagnostic tests → final diagnosis), along with a dual-agent diagnostic framework to enforce adherence to clinical reasoning.

Most existing models either focus on single disease entities or lack explicit mechanisms to differentiate between overlapping symptom etiologies. Furthermore, current LLM-based approaches tend to process clinical inputs passively, without guidance to attend to the most critical etiological reasoning cues for diagnosis. In contrast, our study proposes an Etiology-Aware Attention Steering Framework that directly embeds clinical reasoning knowledge into both the attention mechanism and training objectives of the model. This approach not only improves diagnostic granularity and accuracy but also enhances interpretability by aligning attention behaviors with annotated reasoning elements.

## 3. Methods

This study aims to enhance the diagnostic performance of LLMs in complex emergency settings, specifically focusing on three clinically confusable acute abdominal emergencies: acute appendicitis, acute pancreatitis, and acute cholecystitis. To this end, we propose an Etiology-Aware Attention Steering Framework, designed to improve the model's ability to perform accurate, reasoning-aligned diagnosis in high-ambiguity scenarios. As illustrated in Figure 1, the proposed framework consists of three stages: In the first stage, we constructed CRS based on authoritative diagnostic guidelines for the three target diseases, and subsequently used it to guide the annotation of key reasoning cues and elements within the original patient records. In the second stage, we develop an Etiology-Aware Head Identification algorithm to identify attention heads that align most closely with the annotated reasoning elements, locating internal mechanisms critical to etiological reasoning. In the third stage, we integrate a novel Reasoning-Guided Loss function into a PEFT process using LoRA. This loss function explicitly encourages the identified Etiology-Aware Heads to focus on annotated reasoning elements with the guide of etiological reasoning cues, thereby aligning attention behavior with clinical reasoning. The following subsections provide a detailed description of each stage in the proposed framework.

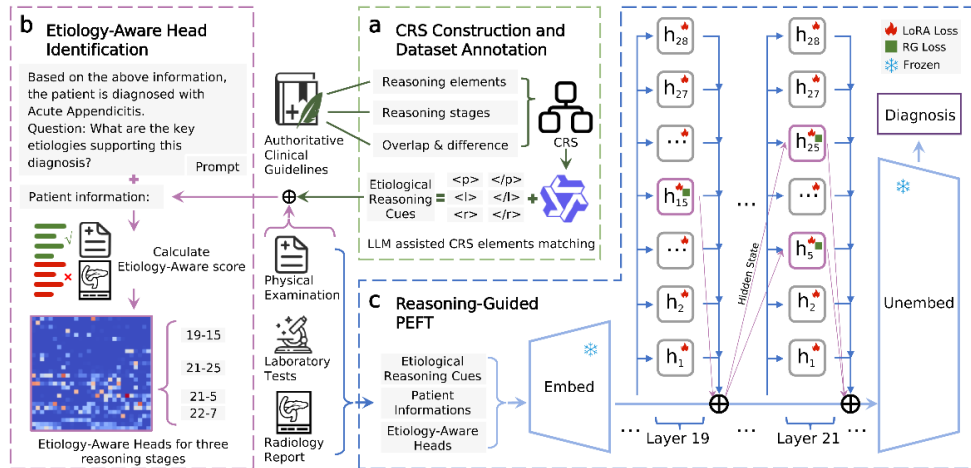


**Figure 1.** The Etiology-Aware Attention Steering Framework. (a) Clinical Reasoning Scaffolding Construction and Dataset Annotation: This stage demonstrates the construction of CRS based on diagnostic guidelines and the use of CRS to annotate reasoning cues and elements in patient records. (b) Etiology-Aware Head Identification: This stage introduces how to identify attention heads aligned with CRS-annotated reasoning elements, pinpointing the internal mechanisms critical to etiological reasoning. (c) Reasoning-Guided Parameter-Efficient Fine-Tuning: This stage shows the integration of a novel Reasoning-Guided Loss function into the PEFT process using LoRA, steering the identified Etiology-Aware Heads to focus on the CRS-annotated reasoning elements, aligning attention behavior with clinical reasoning.

### 3.1. Clinical Reasoning Scaffolding Construction and Dataset Annotation

To guide LLMs in following reliable clinical reasoning paths, we first systematically analyzed authoritative clinical guidelines published in recent years (Kumar et al., 2024; Di Saverio et al., 2020; Moris et al., 2021; Takada et al., 2013, 2007; Yixue Xuehui Waikexue Fenhui Yixian Waikexue Xuezu., 2021; Lankisch et al., 2015). Specifically, we focused on diagnostic procedures for three acute abdominal emergencies—acute appendicitis, acute pancreatitis, and acute cholecystitis—and constructed CRS based on clinical guidelines, which are international or national expert consensuses, characterized by high professional recognition and practical value, covering the mainstream diagnosis and treatment processes for the target diseases. The CRS extracts three key stages from the real-world clinical diagnosis process: physical examination, laboratory tests, and radiology report. Each stage consists of representative reasoning elements. In its design, CRS places special emphasis on the overlap and differences in clinical presentations among the three diseases, aiming to identify etiology through multidimensional clues and ultimately with the goal of reaching a definitive diagnosis. The structure of CRS is as shown in Figure 2.

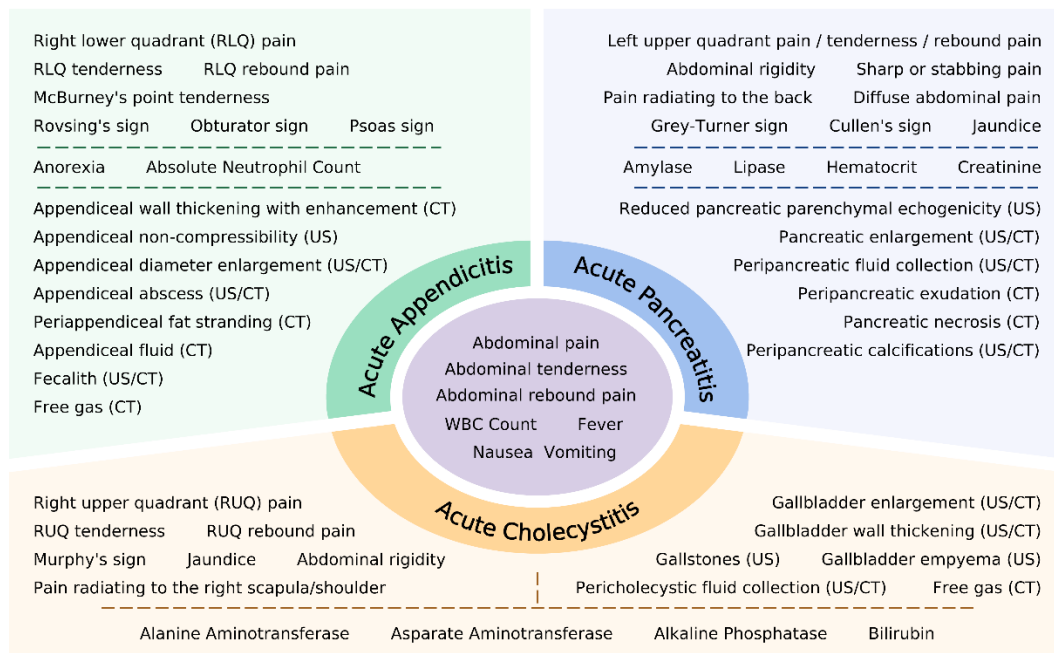


**Figure 2.** Clinical Reasoning Scaffolding derived from authoritative clinical guidelines. For the three target diseases, the CRS defines reasoning elements across physical examination, laboratory tests, and radiology report, offering LLMs a clinically grounded scaffolding for diagnostic reasoning.

To support subsequent tasks of Etiology-Aware Head Identification and Reasoning-Guided PEFT, we annotated patient records based on the following strategy: First, we used a locally deployed LLM (Qwen2.5-32B-Instruct) and designed prompts (see Supplementary Data 1.1) based on the CRS, prompting the model to identify reasoning elements in unstructured clinical narratives. Next, we reviewed and refined the model outputs, correcting conceptual confusions and format inconsistencies, thereby ensuring annotation quality. To enable precise tagging of CRS information, we introduced reasoning tokens as etiological reasoning cues and ensure model can recognize them. For the three reasoning stages, we used dedicated start–end reasoning tokens: `<p>` `</p>` for physical examination, `<l>` `</l>` for laboratory tests, and `<r>` `</r>` for radiology report. Assuming a patient record  $M$  consists

of  $m$  sentences and a sentence  $s_p$  contains  $n$  tokens related to physical examination, the annotation process can be represented in vectorized form (1) (2), where  $t$  denotes an individual token after tokenization.

$$M = \{s_1, s_2, \dots, s_p, \dots, s_l, \dots, s_r, \dots, s_m\} \quad (1)$$

$$s_p = [t_1, t_2, \dots, t_i, \dots, t_j, \dots, t_n] \xrightarrow{\text{note}} s_p = [t_1, t_2, \dots, <p>, t_i, \dots, t_j, </p>, \dots, t_n] \quad (2)$$

The annotation process is completed by adding respective start and end reasoning tokens to the sentences  $s_p$ ,  $s_l$ , and  $s_r$  that contain the three-stage reasoning elements in a patient record.

### 3.2. Etiology-Aware Head Identification

To gain deeper insight into the attention mechanisms of LLMs during diagnostic reasoning and to identify attention heads with strong sensitivity to key reasoning elements, we designed an Etiology-Aware Head Identification algorithm. The core idea of the algorithm is to construct a tailored reasoning-prompting task that guides the model to perform etiological reasoning based on patient records. This enables a systematic analysis of the attention distribution of each head in every transformer layer during token-by-token generation. The etiology in this context refers to the reasoning nodes and indicative cues that support the final diagnosis—namely, the CRS-annotated reasoning elements within the patient records. For each attention head, we compute an Etiology-Aware Score based on the degree to which it attends to these etiology-related tokens. The detailed calculation process is outlined in Algorithm 1.

---

Algorithm 1 Etiology-Aware Head Identification

---

**Input :**

Etiology-Aware Head Identification dataset  $D^I$

Task-specific prompt (see Supplementary Data 1.2)

**Output :**

Etiology-Aware score matrix  $EAS \in \mathbb{R}^{G \times L \times H}$ , where  $G$  is number of reasoning stages (Physical exam, Lab tests,

Radiology),  $L$  is number of model's transformer layers and  $H$  is number of attention heads per layer

**Procedure:**

Initialize  $EAS \leftarrow 0 \in \mathbb{R}^{G \times L \times H}$

**for** each reasoning stage index  $i = 1$  to  $G$  :

**for** each layer index  $j = 1$  to  $L$  :

**for** each head index  $k = 1$  to  $H$  :

**for** each instance  $x \in D^I$  :

                Feed  $x$  and prompt into the model

                Extract the attention score matrix  $A_{j,k}$  for the head  $(j, k)$

                Identify the token index with the maximum attention score

**if** this index lies within the CRS-labeled etiology token range:

                    Increment  $EAS[i][j][k] \leftarrow EAS[i][j][k] + 1$

                Normalize  $EAS[i][j][k]$  by dividing by the number of etiology tokens in stage  $i$

**return**  $EAS$

---

We constructed a prompt template for etiology awareness (Supplementary Data 1.2), guiding the model to generate etiological explanations based on known diagnostic labels. During generation, model's attention maps would significantly focus on certain tokens in the input. For each attention head, we record the positions of its highest attention weights throughout the generation process and determine whether those positions fall within CRS-annotated spans. If so, the head is considered to have successfully captured etiological reasoning cues. To further explore the functional specialization of attention heads across different stages of clinical reasoning, we applied this identification process separately to the three main stages defined in the CRS—physical examination, laboratory tests, and radiology report. This allowed us to quantify the etiology-aware ability of each head and select Etiology-Aware Heads with respect to specific reasoning stages, providing a structured and interpretable foundation for the subsequent Reasoning-Guided PEFT.

### 3.3. Reasoning-Guided Parameter-Efficient Fine-Tuning

To further enhance the model's ability to focus on annotated reasoning elements, we propose a Reasoning-Guided Loss as part of a PEFT strategy, designed to reinforce the model's perception of the etiological reasoning cues throughout the diagnostic task.

We adopt LoRA as the PEFT method. In this approach, the main body of the pre-trained model remains frozen, and only the inserted low-rank matrices are updated during training. For the base loss computation, we apply label smoothing cross-entropy, which mitigates overfitting to hard labels by smoothing the ground truth distribution. Specifically, the true label distribution  $y_i$  is transformed into a smoothed version  $\tilde{y}_i$  using a smoothing factor  $\varepsilon$  and the number of classes  $K$ , and the loss is computed according to Equations (3) and (4).

$$\tilde{y}_i = \begin{cases} 1 - \varepsilon, & i = \text{true label} \\ \frac{\varepsilon}{K - 1}, & \text{others} \end{cases} \quad (3)$$

$$\mathcal{L}_{smooth} = - \sum_i \tilde{y}_i \log p_i \quad (4)$$

Building upon this, we define the Reasoning-Guided Loss to quantify how well the model attends to reasoning elements during prediction. For a given attention head  $H_{l,h}$  with an attention matrix  $A_{l,h}$ , we compute the  $Att(H_{l,h}, s_t)$  for a target reasoning element  $s_t$ , defined as follows:

$$Att(H_{l,h}, s_t) = \frac{\sum_{y=1}^n \sum_{x=i}^j A_{l,h}(x, y)}{\sum_{y=1}^n \sum_{x=i}^n A_{l,h}(x, y)} \quad (5)$$

where the input sequence length is  $n$ , and the attention score matrix  $A_{l,h} \in \mathbb{R}^{n \times n}$ . The indices  $i$  and  $j$  represent the start and end token positions of the target reasoning elements in the input sequence. By accumulating the attention scores within the interval from the  $i$ -th token to the  $j$ -th token and calculating the proportion relative to the total sum of  $A_{l,h}$ , the attention score for the target segment is determined.

During Reasoning-Guided PEFT, we compute these attention scores for all Etiology-Aware Heads over their corresponding CRS-annotated reasoning elements. The final loss function incorporates these scores via a weighted combination with the label smoothing loss, as shown in Equation (6):

$$\mathcal{L}_{RG} = \mathcal{L}_{smooth} + \frac{\lambda}{2} \left(1 + \cos \frac{e\pi}{E}\right) \left[1 - \frac{1}{|H|} \sum_H Att(H, s)\right] \quad (6)$$

where  $\lambda$  is a balancing factor that controls the trade-off between the label smoothing loss and the Reasoning-Guided Loss, while  $e$  and  $E$  denote the current and total training steps, respectively. We apply a cosine decay schedule to modulate the contribution of the Reasoning-Guided Loss over time—assigning greater weight in the early training stages and gradually reducing it to prevent overfitting to specific token spans.

Through this strategy, the model not only learns to generate accurate diagnostic results but also internalizes clinically credible reasoning patterns within its multi-head attention mechanisms. This effectively integrates clinical reasoning into the model's fine-tuning process, achieving unified modeling of both diagnosis generation and etiology reasoning.

## 4. Experiments

### 4.1. Dataset

This study constructed two distinct datasets for evaluating model performance: the Consistent Diagnosis Cohort and the Discrepant Diagnosis Cohort. The former is used to assess the model's diagnostic and reasoning capabilities on clear and structurally complete samples, while the latter evaluates the model's performance in real-world clinical scenarios characterized by missing information and symptom confusion.

For the Consistent Diagnosis Cohort, we utilized clinical data from the MIMIC-IV (v2.2) database (Multiparameter Intelligent Monitoring in Intensive Care) (Johnson, Bulgarelli, Pollard et al., 2023; Johnson, Bulgarelli, Shen et al., 2021; Goldberger et al., 2000), developed and maintained by the Massachusetts Institute of Technology (MIT). This database contains

de-identified electronic health records (EHRs) of nearly 300,000 patients who received inpatient or emergency care at Beth Israel Deaconess Medical Center between 2008 and 2019. The authors completed the necessary ethical training and obtained access permission. During dataset construction, we partially followed the data preprocessing scheme proposed by Hager et al. (2024) for MIMIC-CDM to improve data quality and enhance comparability with previous studies. This scheme involved structured conversion, text cleaning, and diagnostic cohort selection, with the complete work available on GitHub and the PhysioNet platform. The Consistent Diagnosis Cohort focuses on acute appendicitis, acute cholecystitis, and acute pancreatitis, with the initial cohort consisting of patients with one of these as the primary ICD diagnosis upon admission. To ensure clinical completeness, only records with data from physical examinations, laboratory tests, and imaging reports were retained. Samples missing any of these pieces of information were excluded. Additionally, to focus on first-time emergency cases, we further removed records in which the discharge summary explicitly mentioned one of the three target diseases in the present illness section. These records typically belonged to patients who were transferred or had recurrent cases and lacked the necessary initial emergency context. If the discharge diagnosis included a major condition other than the target disease, these records were also excluded. The final cohort included 957 cases of acute appendicitis, 648 cases of acute cholecystitis, and 538 cases of acute pancreatitis. The demographic and clinical characteristics of the Consistent Diagnosis Cohort are shown in Supplementary Data 2.

In contrast, the Discrepant Diagnosis Cohort was specifically constructed to analyze the model's diagnostic reasoning capabilities in cases with clinical inconsistencies between initial and final diagnoses. We used outpatient EHR data from the First Affiliated Hospital, Zhejiang University School of Medicine, spanning from 2010 to 2021, which included all patients with abdominal symptoms. The study was approved by the hospital's Clinical Research Ethics Committee (Approval No. 2022-809). This cohort similarly focused on acute appendicitis, acute cholecystitis, and acute pancreatitis, but selected records where the final diagnosis was one of the target diseases, yet the initial outpatient diagnosis differed. For instance, a patient diagnosed with acute cholecystitis as the final diagnosis might have been initially diagnosed with acute pancreatitis or gallstones. The Discrepant Diagnosis Cohort ultimately included 103 cases of acute appendicitis, 54 cases of acute cholecystitis, and 106 cases of acute pancreatitis. The demographic and clinical characteristics of the Discrepant Diagnosis Cohort are shown in Supplementary Data 2.

#### 4.2. Experimental Setup

To facilitate local deployment and customized training, we selected two open-source models—Qwen2.5-7B-Instruct and DeepSeek-R1-Distill-Qwen-7B—for the tasks of Etiology-Aware Head Identification, Reasoning-Guided PEFT, and model evaluation. Qwen2.5-7B-Instruct is a general-purpose LLM optimized through multi-stage training (Qwen et al., 2025). It is pretrained on over 18 trillion tokens and fine-tuned with more than one million high-complexity task samples via supervised learning and reinforcement learning. It demonstrates strong performance across benchmarks in language understanding, reasoning, mathematics, programming, and human preference alignment. DeepSeek-R1-Distill-Qwen-7B is a lightweight reasoning-specialized model distilled from DeepSeek-R1 using the Qwen architecture (DeepSeek-AI et al., 2025). It preserves the teacher model's strong reasoning capability while significantly reducing the cost of local deployment.

For the Etiology-Aware Head Identification task, we randomly selected 120 patient records for each of the three target diseases to construct disease-specific subsets, along with an additional 40 mixed records sampled from all three diseases. The identification was conducted on a single NVIDIA RTX 4090 GPU. For the Reasoning-Guided PEFT task, we adopted a five-fold cross-validation strategy and optimized hyperparameters to ensure stable and efficient training on a single NVIDIA A100 GPU. The complete experimental code and configuration details are available at: <https://github.com/Twilight-sp/EAS-Diagnosis>.

#### 4.3. Baseline and Evaluation Metrics

We adopted several baseline models for performance benchmarking and method validation, which are categorized as follows:

**Qwen/DeepSeek-distill** refer to the Qwen2.5-7B-Instruct and DeepSeek-R1-Distill-Qwen-7B models, respectively.

**Qwen(LoRA)/DeepSeek-distill(LoRA)** denote the LoRA fine-tuned versions of the above models.

**Qwen(our)/DeepSeek-distill(our)** represent the models fine-tuned using our proposed Reasoning-Guided PEFT approach.

**Llama-70B** refers to the Llama-3.3-70B-Instruct model, reported as the best-performing model in the evaluation of Hager et al. (2024).

To evaluate the base diagnostic capabilities, we adopted common multi-label classification metrics, including: **Overall accuracy**, which reflects the proportion of cases in which all three diseases were correctly identified. **Per-class accuracy (recall)**, which measures the proportion of correctly diagnosed cases within each disease category.

To assess clinical reasoning capability, we introduced the **Reasoning Focus Score**, which quantifies the model's ability to attend to reasoning elements in the input sequence during diagnosis. Additionally, we employed **ROUGE-L F1**, a widely used metric for free-text evaluation, to assess the semantic coherence and preservation of key information in the model-generated reasoning explanations.

To further examine how models focus to semantically meaningful input segments during diagnosis, we introduced the **Reasoning Attention Frequency**. This metric is defined at the segment level: for each semantic segment, we count how many times it is attended to by the model across the entire evaluation dataset, and normalize this count by the total number of occurrences of that segment in the dataset. The resulting value reflects the frequency with which the model focuses on clinically meaningful information during diagnostic reasoning.

#### 4.4. Results in Consistent Diagnosis Cohort

We first conducted Etiology-Aware Head Identification using the Qwen and DeepSeek-distill models on the Consistent Diagnosis Cohort. For each attention head, we calculated the Etiology-Aware Score across three reasoning stages, followed by normalization within balanced mixed subsets containing an equal number of cases from each of the three diseases. The top-10 scoring attention heads in each reasoning stage are visualized in Figure 3, where each vertical axis label  $l-h$  denotes the  $h$ -th head in the  $l$ -th transformer layer.

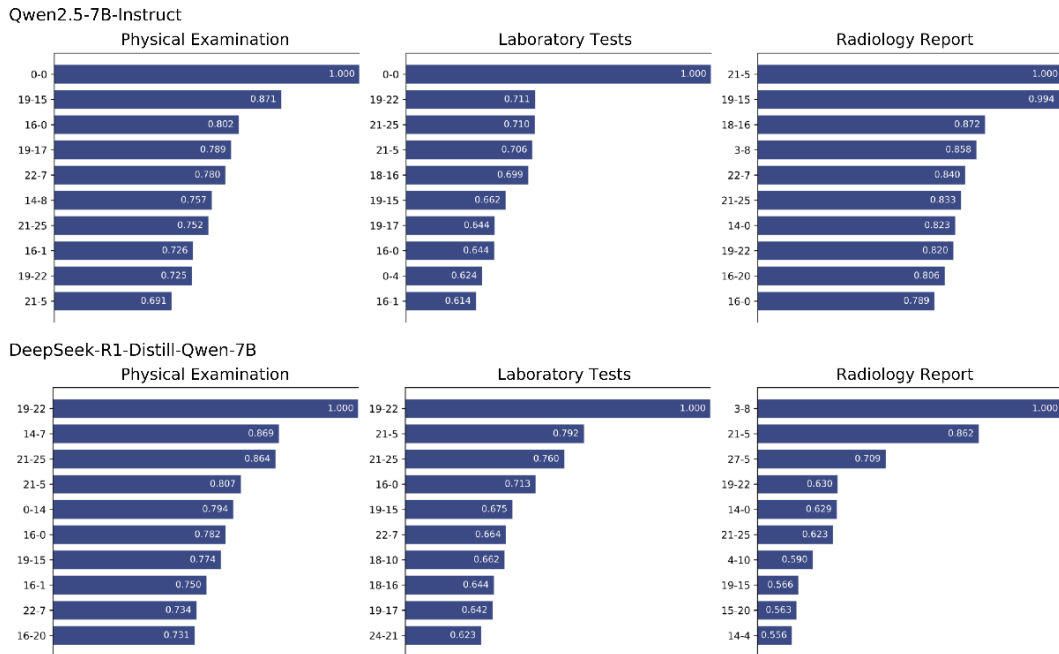


**Figure 3.** Top-10 attention heads ranked by Etiology-Aware Score across three reasoning stages for both models. The test set was constructed using equally mixed cases of the three diseases. Scores were normalized. Vertical labels indicate  $layer-head$  identifiers.

The results show that both Qwen and DeepSeek-distill possess multiple high-scoring attention heads in each reasoning stage. Moreover, some heads exhibit cross-stage consistency. For instance, DeepSeek-distill's head  $19-22$  achieved the highest score in the physical examination stage and also ranked highly in the other two stages, suggesting a potential core role in the overall diagnostic reasoning chain. To assess the consistency of attention mechanisms across different diseases, we further computed the Jaccard similarity matrix between the sets of top-10 attention heads identified separately for each disease. As shown in Figure 4,

Qwen exhibited high inter-disease similarity (mostly >0.8), indicating strong stability and disease-agnostic etiology perception. In contrast, DeepSeek-distill showed more disease-specific attention patterns, particularly in the laboratory tests and radiology report stages, where the overlap between top heads across diseases was relatively low.

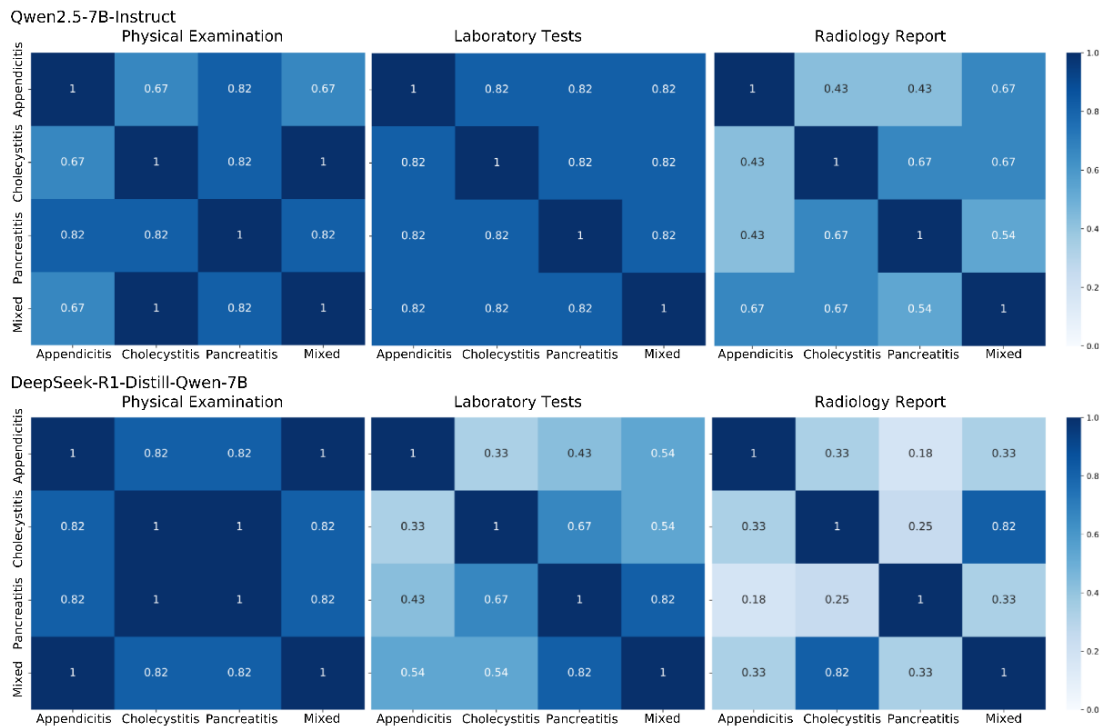


**Figure 4.** Jaccard similarity matrices of top-10 attention heads across different disease-specific subsets. Separate evaluations were conducted on appendicitis-only, cholecystitis-only, pancreatitis-only, and mixed datasets. Scores were normalized prior to computing similarities.

Based on the above analysis, we selected the most prominent attention heads from each model as Etiology-Aware Heads to be used in the Reasoning-Guided PEFT process: For Qwen, heads 19–15 and 21–25 were selected for physical examination and laboratory tests stages, 21–5 and 22–7 for radiology report stage. For DeepSeek-distill, heads 19–22 and 21–5 were selected for physical examination and laboratory tests stages, 3–8 and 27–5 for radiology report stage.

Subsequently, both Qwen and DeepSeek-distill were fine-tuned using LoRA and our proposed Reasoning-Guided strategy. We compared their performance against their respective base models. Figure 5 illustrates the per-disease accuracy and overall accuracy across the three target diseases.

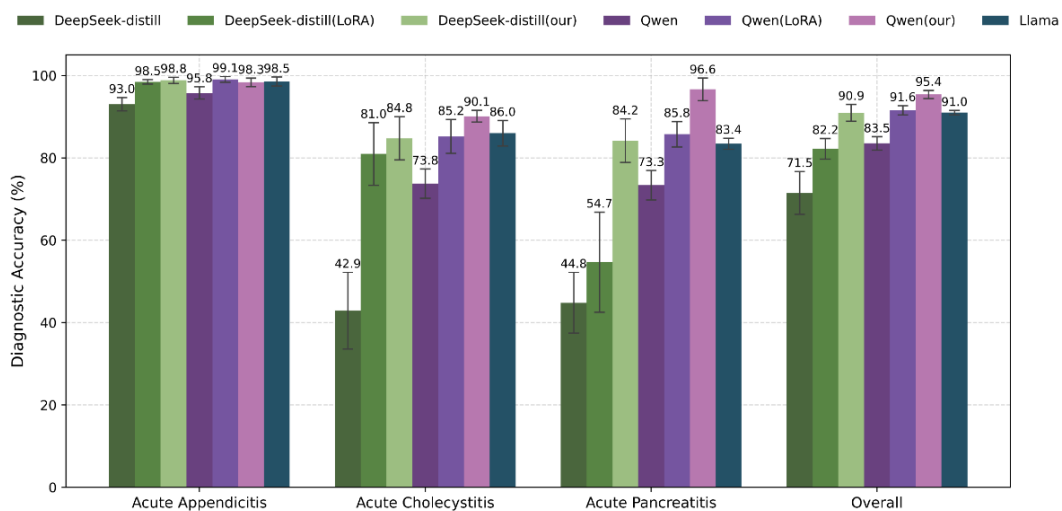


**Figure 5.** Diagnostic accuracy (%) comparison across models in Consistent Diagnosis Cohort. Performance is shown for baseline models, LoRA fine-tuned models (LoRA), and Reasoning-Guided PEFT models (Ours), evaluated both overall and for specific diseases. Error bars indicate 95% confidence intervals derived from five-fold cross-validation using the Z-distribution. Model sizes are as follows: Llama (70B parameters), DeepSeek-distill (7B), and Qwen (7B).

In the base models, Llama performed best in the acute appendicitis task, achieving a diagnostic accuracy of 97.9%. For the more complex and easily confusable conditions of acute cholecystitis and acute pancreatitis, its accuracy declined to 86% and 83.4%, respectively. In contrast, other base models (DeepSeek-distill and Qwen) exhibited further decreases for acute cholecystitis and acute pancreatitis, with the lowest value being DeepSeek's 42.9% for acute cholecystitis. After implementing the LoRA fine-tuning strategy, the performance of models showed widespread improvement. Qwen(LoRA) achieved the highest accuracy rate of 99.1% in the acute appendicitis task. DeepSeek-distill(LoRA) also demonstrated significant enhancement in the acute cholecystitis task, reaching 80%. Upon applying the Reasoning-Guided fine-tuning strategy, all models exhibited further performance gains across three disease diagnostic tasks. Notably, Qwen(our) attained accuracy rates of 90.1% and 96.6% for acute cholecystitis and acute pancreatitis respectively, representing improvements of 15.7% and 23.3% compared to Qwen(LoRA). DeepSeek-distill(our) achieved a 73.3% accuracy rate in the acute pancreatitis task, marking a substantial 29.5% increase over DeepSeek-distill(LoRA).

To evaluate the statistical significance of model performance differences, we conducted one-sided Wilcoxon signed-rank tests. Results revealed statistically significant improvements ( $P = 0.0312 < 0.05$ ) in overall accuracy and per-disease diagnostic accuracy when comparing Qwen(our) with Qwen, and DeepSeek-distill(our) with DeepSeek. Furthermore, when compared with their respective LoRA-fine-tuned versions, both Qwen(RG) and DeepSeek(RG) demonstrated significant gains in overall accuracy and in the tasks of acute cholecystitis and acute pancreatitis ( $P = 0.0312$ ). Detailed results are shown in Supplementary Data 3.

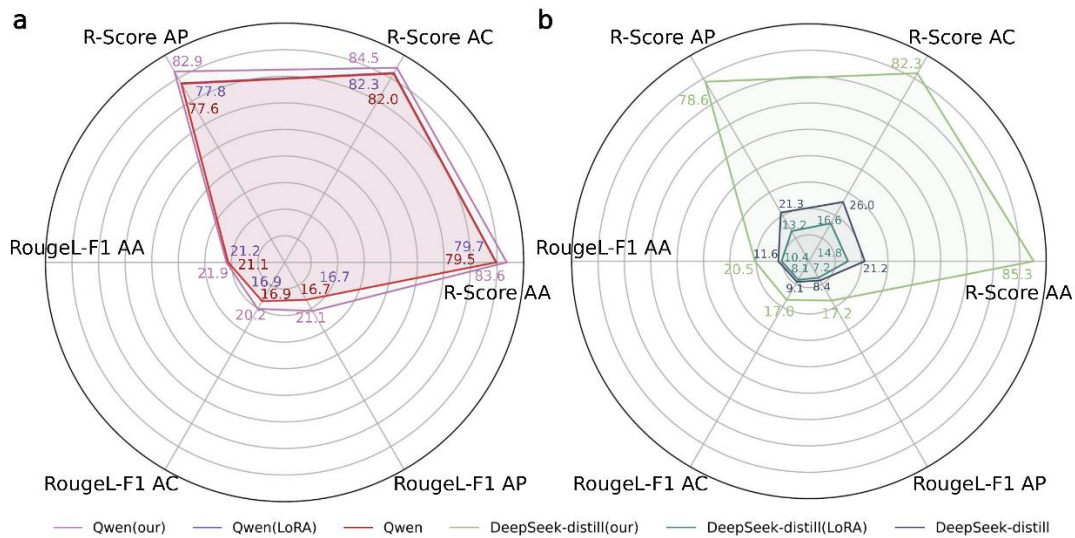


**Figure 6.** Evaluation of reasoning-related metrics. (a) Comparison of three Qwen variants across the three diagnostic tasks. (b) Comparison of three DeepSeek-distill variants. AA: Acute Appendicitis, AC: Acute Cholecystitis, AP: Acute Pancreatitis; R-Score: Reasoning Focus Score; RougeL-F1: F1 score of RougeL.

To further assess each model's reasoning capability during diagnostic generation, we introduced two reasoning-specific evaluation metrics: Reasoning Focus Score, which quantifies the model's attention to input representations by decoding attention maps, reflecting its focus on clinically important clues. RougeL-F1, a standard metric in free-text evaluation, measuring the semantic coherence and preservation of key information in the model's reasoning outputs. As shown in Figure 6a, across all three disease tasks, Qwen(our) consistently achieved the highest R-Scores, indicating that the Reasoning-Guided PEFT effectively enhanced the model's attention to key reasoning elements. For RougeL-F1, Qwen(our) outperformed other versions in acute cholecystitis and acute pancreatitis, though it slightly underperformed the base model in acute appendicitis. Figure 6b presents the results for the DeepSeek-distill series. DeepSeek-distill(our) showed clear and consistent improvements across both metrics compared to the base and LoRA models, especially in R-Score, demonstrating stronger attention focus during reasoning.

Unexpectedly, DeepSeek-distill(LoRA) underperformed the base model across all metrics and tasks, suggesting potential alignment gaps when fine-tuning for reasoning-specialized LLM.

**Table 1.** Experimental results of ablation experiments. AA: Acute Appendicitis, AC: Acute Cholecystitis, AP: Acute Pancreatitis.

Model	Accuracy	Macro-F1	AA Recall	AC Recall	AP Recall
Qwen(our)	<b>0.9542</b>	<b>0.9468</b>	0.9833	0.9011	<b>0.9665</b>
Qwen w/o CRS	0.9156	0.8992	0.9906	0.8521	0.8575
Qwen w/o E-A Head	0.7389	0.6827	0.9427	0.3077	0.8972
Qwen w/o R-G Loss	0.9415	0.9290	<b>0.9948</b>	<b>0.9400</b>	0.8431
DeepSeek-distill(our)	<b>0.9094</b>	<b>0.8938</b>	0.9885	0.8477	<b>0.8420</b>
DeepSeek-distill w/o CRS	0.8221	0.7807	0.9847	0.8096	0.5466
DeepSeek-distill w/o E-A Head	0.7415	0.6684	0.9607	0.7414	0.3034
DeepSeek-distill w/o R-G Loss	0.9021	0.8783	<b>0.9896</b>	<b>0.9462</b>	0.6915

To further validate the effectiveness of Reasoning-Guided FEFT and to investigate the impact of each module on overall performance, we conducted ablation studies focusing on three key components: CRS data annotation, Etiology-Aware Head Identification, and Reasoning-Guided Loss. Specifically, we designed the following three ablation settings: (1) removing the use of annotated data during fine-tuning (w/o CRS); (2) applying Reasoning-Guided Loss uniformly to all attention heads without Etiology-Aware Heads selection (w/o E-A Head); and (3) removing the Reasoning-Guided Loss entirely (w/o R-G Loss). The results are summarized in Table 1. Since the calculation of the Reasoning-Guided Loss depends on the etiological reasoning cues in the annotated data, in the w/o CRS experiment, only the label smoothing cross-entropy loss becomes effective during the training process on the unannotated dataset, yielding training results comparable to those achieved with LoRA fine-tuning. In the w/o E-A Head experiment, since there was no etiology-aware score for attention heads, we manually partitioned them along the transformer layers: the first quarter were assigned to physical examination elements, the next half to radiology report elements, and the remaining quarter to laboratory test elements. In the w/o R-G Loss experiment, we used annotated data, and during training, only the label smoothing cross-entropy loss was computed, without introducing the Reasoning-Guided Loss function. Apart from the aforementioned variables, all other aspects of the model structure and parameter configurations remained consistent throughout the training process.

#### 4.5. Results in Discrepant Diagnosis Cohort

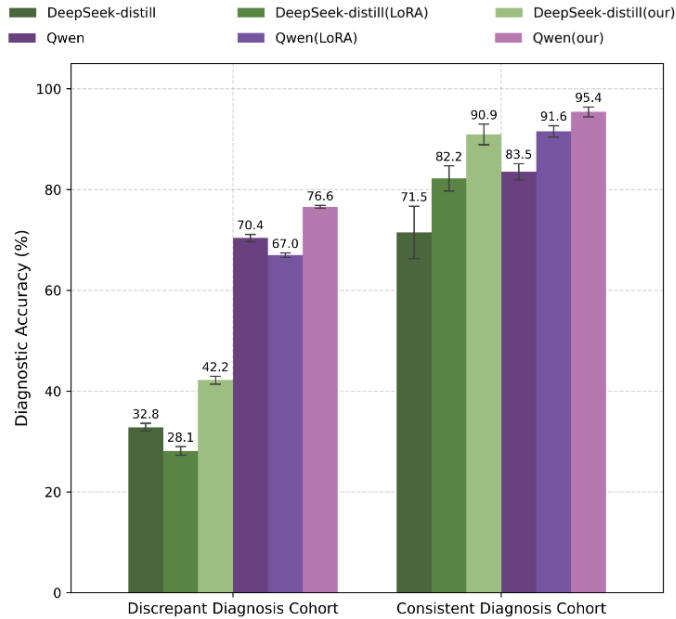


**Figure 7.** Diagnostic accuracy comparison across models in the Discrepant Diagnosis Cohort and Consistent Diagnosis Cohort. Both the LoRA and Ours models were fine-tuned on the Consistent Diagnosis Cohort using LoRA and Reasoning-Guided strategy,

respectively. For external validation on the Discrepant Diagnosis Cohort, the best-performing folds from five-fold cross-validation were selected for each model.

We evaluated the performance of both Qwen and DeepSeek-distill models on the Discrepant Diagnosis Cohort, as well as their variants fine-tuned using Consistent Diagnosis Cohort via LoRA and our proposed Reasoning-Guided PEFT method. The results are shown in Figure 7. As expected, across all models, diagnostic accuracy dropped noticeably compared to the Consistent Diagnosis Cohort, highlighting the increased difficulty of making accurate diagnoses in scenarios characterized by ambiguous symptom presentations and incomplete clinical context. The Qwen achieved an accuracy of 70.1%, while Qwen(LoRA) led to a slight decrease to 66.5%. In contrast, Qwen(our) achieved the highest accuracy of 70.3%, slightly surpassing the original model and demonstrating its stabilizing effect on diagnostic consistency under challenging conditions. The DeepSeek DeepSeek-distill-based models exhibited lower overall performance in this cohort. The DeepSeek-distill achieved 31.6% accuracy, which dropped to 25.8% after LoRA fine-tuning. However, our method significantly improved performance to 41.1%, yielding a nearly 10 percentage point increase, suggesting a more substantial enhancement in reasoning robustness.

To further investigate how different models attend to semantically meaningful information during diagnosis, we analyzed the Reasoning Attention Frequency on the Discrepant Diagnosis Cohort. Specifically, we collected the top-10 most attended tokens for each patient record during diagnosis and mapped these tokens back to their corresponding semantic segment. After filtering out trivial or non-informative segments, we computed the Reasoning Attention Frequency for each semantic segment, defined as the proportion of times it was attended to relative to its total occurrence in the dataset. The results are shown in Figure 8.

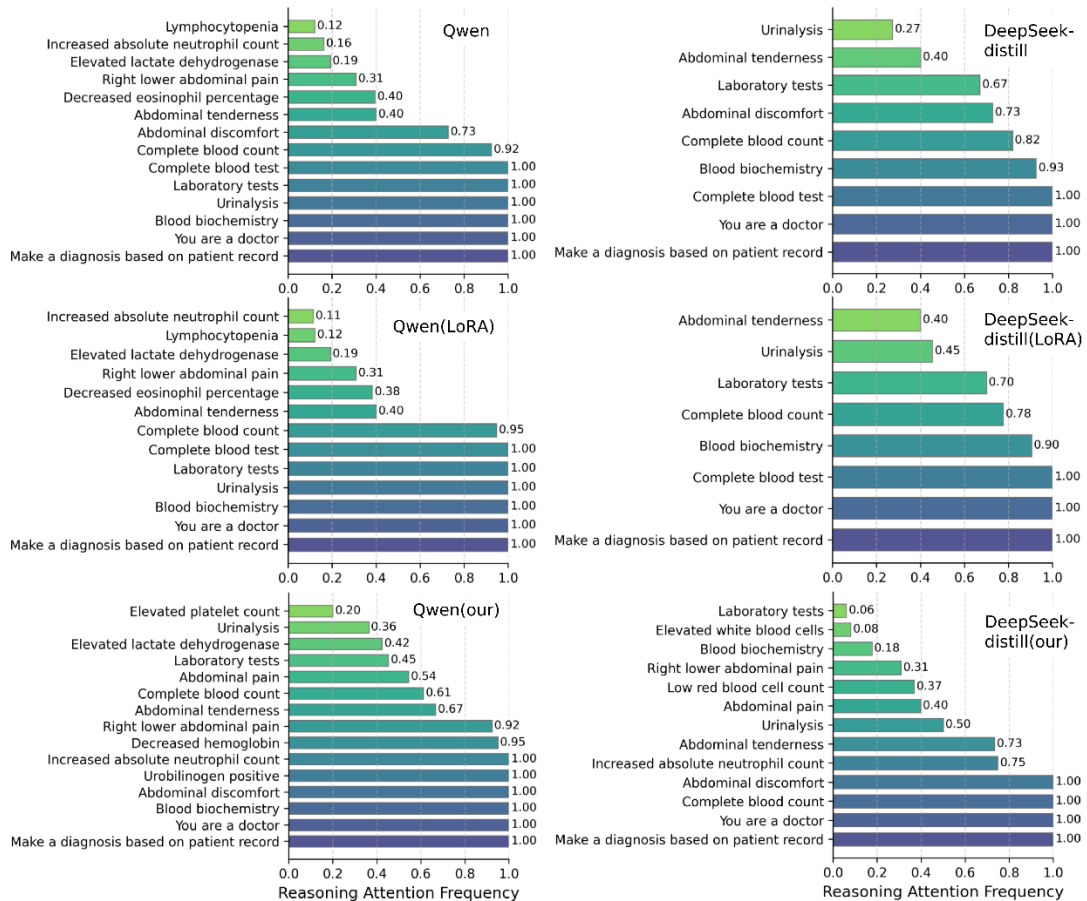


**Figure 8.** Reasoning Attention Frequency across models in the Discrepant Diagnosis Cohort. For each model, the top-10 attended token segments per sample were aggregated and normalized by their total occurrence in the evaluation dataset. This yielded the Reasoning Attention Frequency, indicating how often models focused on clinically relevant tokens during diagnosis.

As illustrated, models fine-tuned with Reasoning-Guided PEFT attend to a richer and more diverse set of meaningful segment, achieving both a higher number of attended semantic segments and greater Reasoning Attention Frequency compared to both base

and LoRA-tuned models. Notably, the base models also outperform their LoRA counterparts in terms of attention to meaningful segments—both in quantity and frequency—echoing the earlier finding that LoRA fine-tuning slightly degrades diagnostic performance on the Discrepant Diagnosis Cohort. This suggests that LoRA tuning may not effectively shift the model's attention to clinically salient cues. In the cross-model comparison, the Qwen-based models demonstrate a broader semantic segment and greater Reasoning Attention Frequency than their DeepSeek-distill counterparts. This aligns with the sharper drop in diagnostic accuracy observed for DeepSeek-distill in the Discrepant Diagnosis Cohort and indicates a lower robustness in capturing diagnostic cues under ambiguous or misleading input contexts.

## 5. Discussion

Evaluation of baseline diagnostic capabilities in Consistent Diagnosis Cohort (Figure 5) revealed that LLMs achieved high accuracy on relatively simple tasks such as acute appendicitis, but their performance significantly declined on more complex diseases like acute cholecystitis and acute pancreatitis. This suggests that untuned general-purpose LLMs struggle with complex clinical tasks requiring the integration of multi-source information and nuanced reasoning. While PEFT via LoRA improved performance, gains were limited in tasks demanding stronger reasoning capabilities. This shows that LoRA prioritizes optimizing label fitting over explicitly enhancing reasoning abilities. In contrast, the proposed Reasoning-Guided PEFT strategy consistently demonstrated superior stability and generalization across all tasks. It explicitly guides the model during fine-tuning to focus on critical etiological reasoning cues, effectively boosting its reasoning and judgment capabilities. For example, Qwen(our) achieved a diagnostic accuracy of 96.6% for acute pancreatitis, significantly outperforming both its base model and the LoRA-finetuned version. These results indicate that reasoning-guided training effectively unlocks the model's potential, markedly enhancing its diagnostic precision and decision-making quality in complex clinical scenarios.

For reasoning capability assessment, the Etiology-Aware Head Identification experiment probed the internal attention mechanisms involved in reasoning. The Qwen model exhibited strong consistency across reasoning stages (physical examination, laboratory tests, radiology report), with some attention heads maintaining high activation scores across multiple stages, suggesting their role in generalized reasoning (Figure 3). This cross-stage attention pattern was confirmed by its Jaccard similarity matrix (Figure 4), which revealed high overlap in attention distributions across different diseases, reflecting Qwen's tendency towards a stable, consistent reasoning. Conversely, the DeepSeek model showed greater attention heterogeneity across diseases, indicating more context-dependent reasoning. Comparative results of reasoning metrics (R-Score and RougeL-F1) aligned well with these observations (Figure 6). Within the Qwen series, Qwen(our) achieved gains in R-Score for all three diseases. While it showed a slight drop in RougeL-F1 for acute appendicitis, significant advantages were evident in acute cholecystitis and pancreatitis. This trend of "enhancing overall reasoning capability at a minimal local cost" reflects improved model adaptability to complex diagnostics. Performance gains from Reasoning-Guided PEFT were even more pronounced in DeepSeek models. Compared to its base model, DeepSeek(our) showed clear improvements in both R-Score and RougeL-F1. In stark contrast, DeepSeek(LoRA) underperformed the base model across all tasks and metrics, abnormally suggesting that LoRA fails to leverage DeepSeek's inherent potential for reasoning-centric tasks. This further underscores the importance of an explicit reasoning guidance mechanism.

Ablation studies (Table 1) provided further confirmation: When Etiology-Aware Head Identification was disabled, model performance dropped considerably across all metrics. Compared to the matching refinement pattern for etiological reasoning cues and Etiology-Aware Heads proposed by us, this reflects that introducing forced attention elements at imprecise locations can cause disturbances in the model's attention. Removing the Reasoning-Guided Loss while retaining the CRS-annotated data—effectively equivalent to a LoRA fine-tuning strategy with annotated supervision—resulted in only a modest decrease in accuracy and macro-F1. However, recall for acute pancreatitis dropped sharply. Given that acute pancreatitis had the fewest samples (acute pancreatitis: 538 vs. acute appendicitis: 957, acute cholecystitis: 648), this suggests that Reasoning-Guided Loss helps maintain diagnostic balance, directing the model to learn fine-grained distinctions among diseases based on reasoning clues—critical for real-world deployment.

The comparative results of diagnostic accuracy between the Diagnosis Divergence Cohort and the Consistent Diagnosis

Cohort (Figure 7) reveal the instability of LoRA in enhancing the diagnostic capabilities of pretrained large language models under certain conditions. Specifically, in scenarios characterized by incomplete clinical information or ambiguous diagnostic tasks, LoRA may suffer from performance degradation due to distributional shifts between the external test dataset and the fine-tuning dataset. In contrast, our proposed Reasoning-Guided PEFT approach introduces the CRS and optimizes the attention mechanism to guide the model in forming more stable attention patterns toward key reasoning elements and etiological reasoning cues during training. This enhances the model's adaptability to complex diagnostic tasks. Notably, in the Diagnosis Divergence Cohort, our method maintains stable accuracy on the Qwen model and achieves significant improvements on the DeepSeek model, demonstrating superior generalizability and robustness compared to LoRA in challenging scenarios. In the Consistent Diagnosis Cohort, our method consistently outperforms LoRA across both models, further validating its ability to enhance clinical reasoning in standard diagnostic settings. In summary, the Reasoning-Guided strategy not only addresses the limitations of LoRA in complex clinical environments but also delivers consistent performance improvements on well-defined tasks, highlighting its broad applicability and clinical potential in the fine-tuning of medical LLMs.

The Reasoning Attention Frequency analysis (Figure 8) reveals that across all models, the system instruction segments (“You are a doctor”, “Make a diagnosis based on patient record”) consistently ranks among the top attended semantic segment. This suggests that models are able to internalize the task prompt and recognize their role in the diagnostic context. More importantly, the Reasoning-Guided PEFT models exhibit stronger attention toward clinically critical diagnostic segments, such as “Right lower abdominal pain”, “Increased absolute neutrophil count”, and “Abdominal discomfort”. In contrast, the base and LoRA-tuned models tend to focus more on general but less informative terms like “Complete blood count” or “Laboratory tests”, which are commonly present but lack specificity for diagnosis. This divergence highlights the value of guided attention: models trained with CRS are more capable of prioritizing key reasoning elements, which in turn enhances diagnostic reasoning. Notably, the Discrepant Diagnosis Cohort is composed of Chinese clinical records, whereas the Reasoning-Guided PEFT was performed using English-language reasoning elements derived from our constructed CRS. Despite the language mismatch, models fine-tuned with our method still aligned their attention with cross-lingual diagnostic reasoning elements, and even surfaced additional plausible cues such as “Decreased hemoglobin” and “Urobilinogen positive”. This suggests that the attention guidance did not overfit the model to a specific language or token pattern, but rather trained it to develop a generalized sensitivity to clinically meaningful content, regardless of expression style or domain variation.

Despite demonstrating the efficacy of Etiology-Aware Attention Steering Framework in enhancing LLMs' reasoning ability, this study has some limitations. First, the CRS used here was manually constructed from clinical guidelines and relied on static reasoning stages and pre-selected attention heads. Its scalability to broader tasks remains to be verified. Second, the selection of reasoning paths was based on heuristics and lacks dynamic adaptability, making it suboptimal for some complex tasks.

Despite demonstrating the effectiveness of the Etiology-Aware Attention Steering Framework in enhancing the reasoning capabilities of LLMs, this study has several limitations. First, the CRS was manually constructed based on clinical guidelines, relying on predefined reasoning stages and pre-selected attention heads, which may limit its scalability to broader diagnostic tasks. Second, the selection of reasoning elements was guided by heuristic rules and lacked dynamic adaptability, potentially rendering it suboptimal for handling more complex or atypical cases.

Nevertheless, this work represents a meaningful advancement in medical LLMs. Our Etiology-Aware Attention Steering Framework approach introduces a structured reasoning attention pathway by identifying and leveraging attention heads that consistently focus on etiological reasoning cues and reasoning elements. This allows the model to explicitly internalize diagnostic reasoning patterns during training, bridging the gap between generation and reasoning. The result is a model that exhibits enhanced focus, improved diagnostic accuracy, and better generalization, surpassing traditional fine-tuning approaches in reasoning-heavy clinical tasks.

Future work may expand this direction along several paths: 1) exploring automated construction of reasoning attention pathways using explainability techniques or reinforcement learning to dynamically identify key reasoning nodes; 2) extending the approach to multi-disease and multi-modal settings; and 3) integrating contrastive or self-supervised objectives to further enhance

model robustness in low-resource or noisy environments.

## 6. Conclusion

This study tackles the challenge of enhancing the clinical reasoning capability and diagnostic performance of LLMs in high-risk scenarios. We propose a novel fine-tuning framework that integrates etiology-aware attention guidance with authoritative clinical guidelines. Extensive experiments demonstrate that our approach significantly improves diagnostic accuracy, attention stability, and reasoning interpretability across diverse tasks. The proposed framework holds strong potential for real-world clinical deployment, particularly in complex and high-stakes diagnostic environments.

## Declaration of competing interest

The authors declare that they have no known competing financial interests or personal relationships that could have appeared to influence the work reported in this paper.

## CRediT author statement

Peixian Li: Investigation, Conceptualization, Methodology, Software, Writing – original draft, Writing – review & editing. Yu Tian: Investigation, Conceptualization, Methodology, Writing – review & editing, Funding acquisition, Project administration. Ruiqi Tu: Software. Chengkai Wu: Methodology. Jingjing Ren: Resources, Data Curation. Jingsong Li: Supervision, Writing – review & editing, Funding acquisition.

## Data availability

The Consistent Diagnosis Cohort is derived from the publicly available MIMIC-IV database. The Discrepant Diagnosis Cohort contains non-public clinical data with data-sharing restrictions.

## Acknowledgments

This work was supported by the National Natural Science Foundation of China (No. 82172069, No. 62402455, No. 72274169), Fundamental Research Funds for the Central Universities (No. 226-2025-00006, No. 226-2024-00163), Innovation and Development Special Fund of Hangzhou West Sci-Tech Innovation Corridor.

## References

- Bhangu, A., Søreide, K., Di Saverio, S., Assarsson, J. H., & Drake, F. T. (2015). Acute appendicitis: Modern understanding of pathogenesis, diagnosis, and management. *The Lancet*, 386(10000), 1278–1287. [https://doi.org/10.1016/S0140-6736\(15\)00275-5](https://doi.org/10.1016/S0140-6736(15)00275-5)
- DeepSeek-AI, Guo, D., Yang, D., Zhang, H., Song, J., Zhang, R., Xu, R., Zhu, Q., Ma, S., Wang, P., Bi, X., Zhang, X., Yu, X., Wu, Y., Wu, Z. F., Gou, Z., Shao, Z., Li, Z., Gao, Z., ... Zhang, Z. (2025). DeepSeek-R1: Incentivizing reasoning capability in LLMs via reinforcement learning. *arXiv*. <https://doi.org/10.48550/arXiv.2501.12948>
- Dettmers, T., Pagnoni, A., Holtzman, A., & Zettlemoyer, L. (2023). QLoRA: Efficient finetuning of quantized llms. *Advances in Neural Information Processing Systems*, (Vol. 36, pp. 10088-10115). <https://doi.org/10.48550/arXiv.2305.14314>
- Di Saverio, S., Podda, M., De Simone, B., Ceresoli, M., Augustin, G., Gori, A., Boermeester, M., Sartelli, M., Coccolini, F., Tarasconi, A., De' Angelis, N., Weber, D. G., Tolonen, M., Birindelli, A., Biffi, W., Moore, E. E., Kelly, M., Soreide, K., Kashuk, J., ... Catena, F. (2020). Diagnosis and treatment of acute appendicitis: 2020 update of the WSES Jerusalem guidelines. *World Journal of Emergency Surgery*, 15(1). <https://doi.org/10.1186/s13017-020-00306-3>
- Ding, N., Qin, Y., Yang, G., Wei, F., Yang, Z., Su, Y., Hu, S., Chen, Y., Chan, C.-M., Chen, W., Yi, J., Zhao, W., Wang, X., Liu, Z., Zheng, H.-T., Chen, J., Liu, Y., Tang, J., Li, J., & Sun, M. (2023). Parameter-efficient fine-tuning of large-scale pre-trained language models. *Nature Machine Intelligence*, 5(3), 220–235. <https://doi.org/10.1038/s42256-023-00626-4>

- Gallagher, J. R., & Charles, A. (2022). Acute cholecystitis: A review. *JAMA*, *327*(10), 965. <https://doi.org/10.1001/jama.2022.2350>
- Gao, Y., Li, R., Croxford, E., Caskey, J., Patterson, B. W., Churpek, M., Miller, T., Dligach, D., & Afshar, M. (2025). Leveraging medical knowledge graphs into large language models for diagnosis prediction: Design and application study. *JMIR AI*, *4*, e58670. <https://doi.org/10.2196/58670>
- Gema, A. P., Jin, C., Abdulaal, A., Diethe, T., Teare, P., Alex, B., Minervini, P., & Saseendran, A. (2024). DeCoRe: Decoding by contrasting retrieval heads to mitigate hallucinations. *arXiv*. <https://doi.org/10.48550/arXiv.2410.18860>
- Goglia, M., Cicolani, A., Carrano, F. M., Petrucciani, N., D'Angelo, F., Pace, M., Chiarini, L., Silecchia, G., & Aurello, P. (2025). Using large language models in the diagnosis of acute cholecystitis: Assessing accuracy and guidelines compliance. *The American Surgeon™*, *91*(6), 967–977. <https://doi.org/10.1177/00031348251323719>
- Goldberger, A., Amaral, L., Glass, L., Hausdorff, J., Ivanov, P. C., Mark, R., ... & Stanley, H. E. (2000). PhysioBank, PhysioToolkit, and PhysioNet: Components of a new research resource for complex physiologic signals. *Circulation [Online]*, *101* (23), pp. e215–e220. RRID:SCR\_007345.
- Hager, P., Jungmann, F., Holland, R., Bhagat, K., Hubrecht, I., Knauer, M., Vielhauer, J., Makowski, M., Braren, R., Kaissis, G., & Rueckert, D. (2024). Evaluation and mitigation of the limitations of large language models in clinical decision-making. *Nature Medicine*, *30*(9), 2613–2622. <https://doi.org/10.1038/s41591-024-03097-1>
- Hao, S., Sukhbaatar, S., Su, D., Li, X., Hu, Z., Weston, J., & Tian, Y. (2024). Training large language models to reason in a continuous latent space. *arXiv*. <https://doi.org/10.48550/arXiv.2412.06769>
- Hu, E. J., Shen, Y., Wallis, P., Allen-Zhu, Z., Li, Y., Wang, S., Wang, L., & Chen, W. (2021). LoRA: Low-Rank adaptation of large language models. *arXiv*. <https://doi.org/10.48550/arXiv.2106.09685>
- Hua, R., Dong, X., Wei, Y., Shu, Z., Yang, P., Hu, Y., Zhou, S., Sun, H., Yan, K., Yan, X., Chang, K., Li, X., Bai, Y., Zhang, R., Wang, W., & Zhou, X. (2024). Lingdan: Enhancing encoding of traditional Chinese medicine knowledge for clinical reasoning tasks with large language models. *Journal of the American Medical Informatics Association*, *31*(9), 2019–2029. <https://doi.org/10.1093/jamia/ocae087>
- Huang, L., Feng, X., Ma, W., Fan, Y., Feng, X., Ye, Y., Zhong, W., Gu, Y., Wang, B., Wu, D., Hu, G., & Qin, B. (2025). Improving contextual faithfulness of large language models via retrieval Heads-Induced optimization. *arXiv*. <https://doi.org/10.48550/arXiv.2501.13573>
- Johnson, A., Bulgarelli, L., Pollard, T., Horng, S., Celi, L. A., & Mark, R. (2023). MIMIC-IV (version 2.2). PhysioNet. RRID:SCR\_007345. <https://doi.org/10.13026/6mm1-ek67>
- Johnson, A., Bulgarelli, L., Shen, L., Gayles, A., Shammout, A., Horng, S., ... & Mark, R. G. (2023). MIMIC-IV, a freely accessible electronic health record dataset. *Scientific data*, *10*(1), 1. <https://doi.org/10.1038/s41597-022-01899-x>
- Krešević, S., Giuffrè, M., Ajčević, M., Accardo, A., Crocè, L. S., & Shung, D. L. (2024). Optimization of hepatological clinical guidelines interpretation by large language models: A retrieval augmented generation-based framework. *npj Digital Medicine*, *7*(1), 102. <https://doi.org/10.1038/s41746-024-01091-y>
- Kumar, S. S., Collings, A. T., Lamm, R., Haskins, I. N., Scholz, S., Nepal, P., Train, A. T., Athanasiadis, D. I., Pucher, P. H., Bradley, J. F., Hanna, N. M., Quinteros, F., Narula, N., & Slater, B. J. (2024). SAGES guideline for the diagnosis and treatment of appendicitis. *Surgical Endoscopy*, *38*(6), 2974–2994. <https://doi.org/10.1007/s00464-024-10813-y>
- Kwon, T., Ong, K. T., Kang, D., Moon, S., Lee, J. R., Hwang, D., Sim, Y., Sohn, B., Lee, D., & Yeo, Young. (2024). Large language models are clinical reasoners: Reasoning-Aware diagnosis framework with Prompt-Generated rationales. In *Proceedings of the AAAI Conference on Artificial Intelligence* (Vol. 38, No. 16, pp. 18417-18425). <https://doi.org/10.1609/aaai.v38i16.29802>
- Lankisch, P. G., Apte, M., & Banks, P. A. (2015). Acute pancreatitis. *The Lancet*, *386*(9988), 85–96. [https://doi.org/10.1016/S0140-6736\(14\)60649-8](https://doi.org/10.1016/S0140-6736(14)60649-8)
- Li, J., Chen, X., Zhou, H., Yi, H., You, M., Liu, W., Wang, L., Li, H., Zhang, X., Guo, Y., Fan, L., Lao, Q., Fu, W., & Li, K. (2025). Grounding large language model in clinical diagnostics. In Review. <https://doi.org/10.21203/rs.3.rs-6286021/v1>

- Liu, X., Liu, H., Yang, G., Jiang, Z., Cui, S., Zhang, Z., Wang, H., Tao, L., Sun, Y., Song, Z., Hong, T., Yang, J., Gao, T., Zhang, J., Li, X., Zhang, J., Sang, Y., Yang, Z., Xue, K., ... Wang, G. (2025). A generalist medical language model for disease diagnosis assistance. *Nature Medicine*, *31*(3), 932–942. <https://doi.org/10.1038/s41591-024-03416-6>
- Ma, Y., Luo, M., Guan, G., Liu, X., Cui, X., & Luo, F. (2025). An explainable predictive machine learning model of gangrenous cholecystitis based on clinical data: A retrospective single center study. *World Journal of Emergency Surgery*, *20*(1). <https://doi.org/10.1186/s13017-024-00571-6>
- Males, I., Boban, Z., Kumric, M., Vrdoljak, J., Berkovic, K., Pogorelic, Z., & Bozic, J. (2024). Applying an explainable machine learning model might reduce the number of negative appendectomies in pediatric patients with a high probability of acute appendicitis. *Scientific Reports*, *14*(1). <https://doi.org/10.1038/s41598-024-63513-x>
- Moris, D., Paulson, E. K., & Pappas, T. N. (2021). Diagnosis and management of acute appendicitis in adults: A review. *JAMA*, *326*(22), 2299. <https://doi.org/10.1001/jama.2021.20502>
- Qwen, Yang, A., Yang, B., Zhang, B., Hui, B., Zheng, B., Yu, B., Li, C., Liu, D., Huang, F., Wei, H., Lin, H., Yang, J., Tu, J., Zhang, J., Yang, J., Yang, J., Zhou, J., Lin, J., ... Qiu, Z. (2025). Qwen2.5 technical report. *arXiv*. <https://doi.org/10.48550/arXiv.2412.15115>
- Savage, T., Nayak, A., Gallo, R., Rangan, E., & Chen, J. H. (2024). Diagnostic reasoning prompts reveal the potential for large language model interpretability in medicine. *npj Digital Medicine*, *7*(1), 20. <https://doi.org/10.1038/s41746-024-01010-1>
- Shah-Mohammadi, F., & Finkelstein, J. (2024). Accuracy evaluation of GPT-Assisted differential diagnosis in emergency department. *Diagnostics*, *14*(16), 1779. <https://doi.org/10.3390/diagnostics14161779>
- Shen, Z., Yan, H., Zhang, L., Hu, Z., Du, Y., & He, Y. (2025). CODI: Compressing Chain-of-Thought into continuous space via Self-Distillation. *arXiv*. <https://doi.org/10.48550/arXiv.2502.21074>
- Singhal, K., Azizi, S., Tu, T., Mahdavi, S. S., Wei, J., Chung, H. W., Scales, N., Tanwani, A., Cole-Lewis, H., Pfohl, S., Payne, P., Seneviratne, M., Gamble, P., Kelly, C., Babiker, A., Schärli, N., Chowdhery, A., Mansfield, P., Demner-Fushman, D., ... Natarajan, V. (2023). Large language models encode clinical knowledge. *Nature*, *620*(7972), 172–180. <https://doi.org/10.1038/s41586-023-06291-2>
- Sonoda, Y., Kurokawa, R., Hagiwara, A., Asari, Y., Fukushima, T., Kanzawa, J., Gono, W., & Abe, O. (2024). Structured clinical reasoning prompt enhances LLM's diagnostic capabilities in diagnosis please quiz cases. *Japanese Journal of Radiology*, *43*(4), 586–592. <https://doi.org/10.1007/s11604-024-01712-2>
- Takada, T., Kawarada, Y., Nimura, Y., Yoshida, M., Mayumi, T., Sekimoto, M., Miura, F., Wada, K., Hirota, M., Yamashita, Y., Nagino, M., Tsuyuguchi, T., Tanaka, A., Kimura, Y., Yasuda, H., Hirata, K., Pitt, H. A., Strasberg, S. M., Gadacz, T. R., ... Liao, K.-H. (2007). Background: Tokyo Guidelines for the management of acute cholangitis and cholecystitis. *Journal of Hepato-Biliary-Pancreatic Surgery*, *14*(1), 1–10. <https://doi.org/10.1007/s00534-006-1150-0>
- Takada, T., Strasberg, S. M., Solomkin, J. S., Pitt, H. A., Gomi, H., Yoshida, M., Mayumi, T., Miura, F., Gouma, D. J., Garden, O. J., Büchler, M. W., Kiriya, S., Yokoe, M., Kimura, Y., Tsuyuguchi, T., Itoi, T., Gabata, T., Higuchi, R., Okamoto, K., ... Sumiyama, Y. (2013). TG13: Updated Tokyo Guidelines for the management of acute cholangitis and cholecystitis. *Journal of Hepato-Biliary-Pancreatic Sciences*, *20*(1), 1–7. <https://doi.org/10.1007/s00534-012-0566-y>
- Vaswani, A., Shazeer, N., Parmar, N., Uszkoreit, J., Jones, L., Gomez, A. N., Kaiser, Ł., & Polosukhin, I. (2017). Attention is all you need. *Advances in Neural Information Processing Systems*, (Vol. 30, pp. 5998–6008). <https://doi.org/10.48550/arXiv.1706.03762>
- Venkateswaran, P., & Contractor, D. (2025). Spotlight your instructions: Instruction-following with dynamic attention steering. *arXiv*. <https://doi.org/10.48550/ARXIV.2505.12025>
- Wang, J., Shue, K., Liu, L., & Hu, G. (2025). Preliminary evaluation of ChatGPT model iterations in emergency department diagnostics. *Scientific Reports*, *15*(1), 10426. <https://doi.org/10.1038/s41598-025-95233-1>
- Wei, J., Wang, X., Schuurmans, D., Bosma, M., Ichter, B., Xia, F., Chi, E., Le, Q. V., & Zhou, D. (2022). Chain-of-Thought

- prompting elicits reasoning in large language models. *Advances in Neural Information Processing Systems*, (Vol. 35, pp. 24824–24837). <https://doi.org/10.48550/arXiv.2201.11903>
- Williams, C. Y. K., Miao, B. Y., Kornblith, A. E., & Butte, A. J. (2024). Evaluating the use of large language models to provide clinical recommendations in the emergency department. *Nature Communications*, 15(1), 8236. <https://doi.org/10.1038/s41467-024-52415-1>
- Williams, C. Y. K., Zack, T., Miao, B. Y., Sushil, M., Wang, M., Kornblith, A. E., & Butte, A. J. (2024). Use of a large language model to assess clinical acuity of adults in the emergency department. *JAMA Network Open*, 7(5), e248895. <https://doi.org/10.1001/jamanetworkopen.2024.8895>
- Wu, J., Deng, W., Li, X., Liu, S., Mi, T., Peng, Y., Xu, Z., Liu, Y., Cho, H., Choi, C.-I., Cao, Y., Ren, H., Li, X., Li, X., & Zhou, Y. (2025). MedReason: Eliciting factual medical reasoning steps in LLMs via knowledge graphs. *arXiv*. <https://doi.org/10.48550/arXiv.2504.00993>
- Wu, J., Wu, X., & Yang, J. (2024). Guiding clinical reasoning with large language models via knowledge seeds. *arXiv*. <http://arxiv.org/abs/2403.06609>
- Wu, W., Wang, Y., Xiao, G., Peng, H., & Fu, Y. (2024). Retrieval head mechanistically explains Long-Context factuality. *arXiv*. <http://arxiv.org/abs/2404.15574>
- Xiao, G., Tang, J., Zuo, J., Guo, J., Yang, S., Tang, H., Fu, Y., & Han, S. (2024). DuoAttention: Efficient Long-Context LLM inference with retrieval and streaming Heads. *arXiv*. <http://arxiv.org/abs/2410.10819>
- Xu, T., Chen, L., Hu, Z., & Li, B. (2025). STAF-LLM: A scalable and task-adaptive fine-tuning framework for large language models in medical domain. *Expert Systems with Applications*, 281, 127582. <https://doi.org/10.1016/j.eswa.2025.127582>
- Yan, Y., Yu, H., Wang, D., Ye, J., Liu, F., & Xu, W. (2025). STP: Special token prompt for parameter-efficient tuning of pre-trained language models. *Expert Systems with Applications*, 284, 127665. <https://doi.org/10.1016/j.eswa.2025.127665>
- Zhang, Q., Chen, M., Bukharin, A., Karampatziakis, N., He, P., Cheng, Y., Chen, W., & Zhao, T. (2023). AdaLoRA: Adaptive budget allocation for Parameter-Efficient Fine-Tuning. *arXiv*. <https://doi.org/10.48550/arXiv.2303.10512>
- Zheng, Z., Wang, Y., Huang, Y., Song, S., Yang, M., Tang, B., Xiong, F., & Li, Z. (2025). Attention heads of large language models. *Patterns*, 6(2), 101176. <https://doi.org/10.1016/j.patter.2025.101176>
- Chinese Pancreatic Surgery Association, Chinese Society of Surgery, Chinese Medical Association. (2021). Guidelines for diagnosis and treatment of acute pancreatitis in China (2021). *Chinese Journal of Surgery*, 59(7), 578–587. <https://doi.org/10.3760/cma.j.cn112139-20210416-00172>

## Appendix. Supplementary Data

### 1 Prompt Template

#### 1.1 Prompt Template for Dataset Annotation

In the prompt template below, {CRS} is reasoning elements in the clinical reasoning scaffolding, and {Information} is the patient records.

```
Please determine whether each symptom in the Clinical Thinking Scaffolding is present in the patient information, following the format strictly:  
- If present, output "Symptom Name: Yes + Original Description"  
- If absent, output "Symptom Name: No"  
Do not add analysis, summaries, or other content. Only output the judgment results for the Clinical Thinking Scaffolding.  
Clinical Thinking Scaffolding:  
{CRS}  
Patient Information:  
{Information}  
Example Output:  
Abdominal pain: Yes + complains of severe abdominal pain  
Right upper quadrant(RLQ) tenderness: No
```

#### 1.2 Prompt Template for Etiology-Aware Head Identification

In the prompt template below, {Information} is the patient records, and {Diagnosis} is the diagnosis result corresponding to the record.

```
Patient information:{Information}  
Based on the above information, the patient is diagnosed with {Diagnosis}.  
Question: What are the key etiologies supporting this diagnosis?  
Answer:
```

## 2 Wilcoxon signed-rank tests results

Consistent Diagnosis Cohort and Discrepant Diagnosis Cohort both contained de-identified patient data, and therefore did not include basic patient characteristics such as age or sex. Table A.1 and Table A.2 present patient characteristics that accounted for  $\geq 5\%$  within each cohort. In the table, '(H)' and '(L)' indicates an abnormal result (higher or lower than the reference range) for the indicator, while '(--)' indicates the indicator is within the normal reference range.

Table A.1. Demographic and Clinical Characteristics of in Consistent Diagnosis Cohort

	Consistent Diagnosis Cohort(n = 2143)
Abdominal pain	2069(96.55%)
Abdominal tenderness	1761(82.17%)
Abdominal rebound pain	157(7.33%)
Fever	588(27.44%)
Vomiting	959(44.75%)
Nausea	1481(69.11%)
Right lower quadrant (RLQ) pain	871(40.64%)
RLQ tenderness	793(37.00%)
RLQ rebound pain	110(5.13%)

Rovsing's sign	123(5.74%)
Anorexia	623(29.49%)
Right upper quadrant (RUQ) pain	759(35.42%)
RUQ tenderness	693(32.34%)
Murphy's sign	137(6.39%)
Epigastric pain	844(39.38%)
Diffuse abdominal pain	406(18.95%)
Dull pain	155(7.23%)
Sharp or stabbing pain	559(26.08%)
Pain radiating to the back	326(15.21%)
Persistent distending pain	232(10.83%)
White Blood Cells (H)/(--)	1370(63.93%) / 771(35.98%)
Absolute Neutrophil Count (H)/(--)	548(25.57%) / 153(7.14%)
Neutrophils (H)/(--)	1649(76.95%) / 455(12.23%)
Alanine Aminotransferase (H)/(--)	626(29.21%) / 1205(56.23%)
Aspartate Aminotransferase (H)/(--)	648(30.24%) / 1185(55.30%)
Alkaline Phosphatase (H)/(--)	416(19.41%) / 1400(65.33%)
Bilirubin (H)/(--)	340(15.87%) / 1480(69.06%)
Amylase (H)/(--)	226(10.55%) / 257(11.99%)
Lipase (H)/(--)	599(27.95%) / 1137(53.06%)
Hematocrit (H)/(--)	1087(50.72%) / 1054(49.18%)
Urea Nitrogen (H)/(--)	441(20.58%) / 1700(79.33%)
Creatinine (H)/(--)	291(12.58%) / 1850(86.33%)
Appendiceal diameter enlargement (US)	719(33.55%)
Appendiceal diameter enlargement (CT)	849(39.62%)
Appendiceal wall thickening with enhancement (CT)	444(20.72%)
Fecalith (CT)	246(11.48%)
Periappendiceal fat stranding (CT)	703(32.80%)
Appendiceal fluid (CT)	158(7.37%)
Gallbladder enlargement (US)	531(24.78%)
Gallbladder enlargement (CT)	270(12.60%)
Gallbladder wall thickening (US)	431(20.11%)
Gallbladder wall thickening (CT)	198(9.24%)
Gallstones (US)	787(36.72%)
Pericholecystic fluid collection/abscess (US)	221(10.31%)
Pericholecystic fluid collection/abscess (CT)	178(8.31%)

Table A.2. Demographic and Clinical Characteristics of in Discrepant Diagnosis Cohort

	Discrepant Diagnosis Cohort(n = 263)
Abdominal pain	63(23.95%)
Abdominal tenderness	41(15.59%)
Abdominal discomfort	17(6.46%)
Right lower quadrant pain	14(5.32%)
Nausea	14(5.32%)

Hyponatremia	34(12.93%)
Hypokalemia	18(6.84%)
Absolute neutrophil count (H)	123(46.77%)
Neutrophil (H)	113(42.97%)
Lymphocyte percentage (L)	124(47.15%)
Lymphocytopenia (L)	33(12.55%)
White blood cells (H)	112(42.59%)
Absolute monocyte count (H)	21(7.98%)
Monocyte percentage (L)	27(10.27%)
Hypochloremia	17(6.46%)
Serum total bilirubin (H)	17(6.46%)
Direct bilirubin (H)	19(7.22%)
Eosinophil percentage (L)	81(30.80%)
Thrombocytopenia	17(6.46%)
Plateletcrit (H)	20(7.60%)
Hemoglobin (L)	20(7.60%)
Mean corpuscular hemoglobin concentration (H)	15(5.70%)
Red blood cell count (L)	19(7.22%)
Hematocrit (L)	23(8.75%)
Lactate dehydrogenase (H)	26(9.89%)
Serum aminotransferases (H)	15(5.70%)
Activated partial thromboplastin time (L)	20(7.60%)
Serum amylase (H)	60(22.81%)
Lipase (H)	56(21.29%)
Aspartate aminotransferase (H)	17(6.46%)

### 3 Wilcoxon signed-rank tests results

Table A.3 presents the One-sided Wilcoxon Signed Ranks Test results comparing models trained with our method against their respective baseline models and models trained using the LoRA fine-tuning approach. The models underwent five-fold cross-validation.

Table A.3. One-sided Wilcoxon Signed Ranks Test Results

	Qwen(our) vs Qwen(LoRA)	Qwen(our) vs Qwen	DeepSeek-distill (our) vs DeepSeek-distill (LoRA)	DeepSeek-distill (our) vs DeepSeek-distill
Overall	P = 0.0312	P = 0.0312	P = 0.0312	P = 0.0312
Acute Appendicitis	P = 0.8438	P = 0.0312	P = 0.0625	P = 0.0312
Acute Cholecystitis	P = 0.0312	P = 0.0312	P = 0.0312	P = 0.0312
Acute Pancreatitis	P = 0.0312	P = 0.0312	P = 0.0312	P = 0.0312